STRUCTURAL SETUP

4.1. GENERAL

As mentioned in the Chapter 3 geologically the area under study is characterised by two distinct lithological units viz. 1) High grade gneisses and schists and 2) Crystalline limestones, quartzites, manganiferous and ferruginous quartzite. The former is designated as of *Pre-Champaner Gneiss* and the latter as *Champaner Group.* These two groups have been intruded by Godhra Granite. Structural Complexity in Goidia, Wawadi, Luni, Chhota Udepur, Longami and Moti Sadli area within Pre-Champaner Gneisses is revealed in the satellite imageries (**Fig.3.1a**), regional lineament map (**Fig 3.1b**), and geological map (**Fig.3.2**). The information in this regard is also supported by structural data and detailed mapping in selected areas. These areas are denoted as different sectors with variable orientation of structural elements. The rocks of Pre-Champaner Gneisses were regionally correlated with the Banded Gneissic Complex. Table 4.1. gives a brief account of the structural elements described by earlier workers.

Pre-Champaner Gneisses have undergone four episodes of deformations namely $\mathbf{D_1}$, $\mathbf{D_2}$, $\mathbf{D_3}$ and $\mathbf{D_4}$ and related folding which are denoted as $\mathbf{F_1}$, $\mathbf{F_2}$, $\mathbf{F_3}$ and $\mathbf{F_4}$ whereas the overlying Champaner Group has experienced the last two episodes of foldings ($\mathbf{F_3}$ and $\mathbf{F_4}$) which may also be redesignated as $\mathbf{CF_1}$ and $\mathbf{CF_2}$.

During the present work, a detailed structural history of Pre-Champaner Gneisses has been brought out with the help of different structural elements. Correlation of these elements with different generation of structural events and analyses of structural data has helped to interpret the probable mechanism of foldings.

LISS III satellite imagery data reveals that there are two sets of fracture, which are regionally present in this area (**Fig. 3.1a**). Structural complexity of the study area is revealed in the regional lineament pattern (**Fig 3.1.b**). By and large two sets of strong lineaments along WNW- ESE and WSW-ENE are present in the study area. The granite gneiss exhibits the WNW- ESE trending lineament that also propagates into the limestone country indicating its post-Champaner time development. However, in the intrusive Godhra Granite the ESE-WNW trending lineament is not well exhibited in the map. Closely spaced curvilinear feature is the characteristic feature of regional folds, which are described below in detail. By and large it can be established that the regional fold pattern is the manifestation of D_3 episode. Table 4.1 shows different views of the early and present workers about folding episodes in Champaner Fold Belt. .

Table 4.1 Table showing different views regarding folding episodes in Champaner Fold Belt

	Heron and Ghosh, 1934.	*Jambusaria 1970*	*Gopinath et al. 1977.*	*Srikarni and Das, 1999.*	*Karanth and Das 2000.*
Champaner Group	Simple	One phase	One phase CF_2, upright folds with E-W axial trace	Two Phases CF_1=upright folds with WNW-ESE axial trace CF_2=upright warps with N-S axial trace.	Two Phases CF_1=upright folds with WNW-ESE axial trace CF_2=upright warps with N-S axial trace.
Pre-Champaner	Not described	Not described	Two phases	Three phases F_1= isoclinal reclined folds, Latest two phases (*F2* and F_3) are common with Champaner Group	Four Phases F_1= isoclinal reclined folds F_2= isoclinal reclined folds with high angles between F_1 (~N-S) and F_2 (~E-W) axes. Later two phases (F_3 &F_4) are common with Champaner Group

4.2.STRUCTURAL ELEMENTS

Structural elements have been recognized on the macroscopic and mesoscopic scales, which have also been supplemented by microscopic studies. The Pre-Champaner Gneisses as described above have undergone four episodes of foldings, which are denoted as F_1, F_2, F3 and F_4 The primary bedding and laminations are denoted as S_0, whereas the axial plane cleavage of F_1, F_2, F_3 and F_4 folds are denoted as S_1, S_2, S_3 and S_4. Different structural elements and related deformation and metamorphic episodes are tentatively correlated and are shown here in **Table 4.2.**

4.2.1 Bedding and lamination

The conspicuous primary structure is the bedding, which can be recognized in ferruginous and micaceous quartzite of Goidia area. Here thin conglomerate beds are also seen interbanded with quartzite showing distinct formational contact (bedding planes). In most of other places it is difficult to recognize the bedding planes.

Table 4.2 showing deformational and metamorphic events of the area under study.

Deformation	Fold Geometry	Nature and Orientation of the fold axis /axial plane	Related metamorphism
D_1	F_1: isoclinal reclined folds with thickened hinges	L_1: represented as mesoscopic fold axes, mineral lineation, plunging towards S or N (variable, but mainly low).	M_1:(Upper Amphibolite Facies) with, kyanite/sillimanite, muscovite, biotite, garnet. metamorphism reached peak.
D_2	F_2: isoclinal reclined folds with thickened hinges	L_2: represented as mesoscopic fold axis lineation, intersection lineation, plunging mainly towards W (10 to 25°).	M_2: (Lower Amphibolite Facies), formation of cordierite -a decompression reaction.
D_3	F_3: upright open to close folds	L_3: occurs both as pucker axis lineation and mineral lineation, plunging 5° to 25° mainly towards W	M_3: (Greenschist Facies) with muscovite, biotite, chlorite.
D_4	F_4: Broad open folds and kink bands	L_4: represented as kink axes plunging 3° to 10° towards N or S.	Contact Metamorphism related to intrusion of Godhra Granite (Local).

4.2.2. Schistosity and gneissosity

Dominant foliation of the pelitic schists in the study area is S_2 and often both S_1 and S_2 are recognizable. S_1 is the axial plane schistosity/cleavage of F_1 folds whereas S_2 is the cleavage formed on account of F_2 folds. Both S_1 and S_2 are low dipping planar surfaces. S_1 is seen to have developed as closely spaced schistosity in mica schist (±kyanite / sillimanite/garnet) and as gneissic bands in quartz–mica gneiss and granite gneiss, whereas in micaceous quartzite it is occurring more or less as fracture cleavage. Only at very few places F_1 refolded on F_2 is recognisable.(e.g. Luni area). In other places recrystallisation along later schistosity (S_2) dominates and the traces of F_1/S_1 is not recognisable. Spacing between schistosity (M-domain) surfaces in S_1 is in the range of 0.1-0.2 mm in quartz-mica schist, 0.2-0.4 mm in garnetiferous biotite schist and 0.5-1 mm in garnetiferous feldspathic gneiss bands. S_2 schistosity and gneissosity are parallel to axial plane of F_2 folds, occurring mostly as crenulation cleavage cutting across S_1 At many places near F_2 hinges it is seen that S_1 has been partially transposed by S_2. Spacing between two mica-rich layers in S_2 is in the range of 1 to 3 mm. S_3 surface is generally steeply dipping and also occurs as crenulation cleavage affecting F_3 hinges. However, transposition of S_2 by S_3 is less intense than that of S_1 by S_2. S_4 is a wide spaced sub-vertical plane occurs parallel to the axial plane of F_4 warps. These are far less penetrative and only recorded in the quartz -muscovite gneiss and pelitic schists

Based on the classification of Powell (1979) the morphological characters of rock cleavage /schistosity are described here. The S_1 could be assigned as *continuous penetrative axial plane cleavage* as well as strong fracture cleavage. S_2 schistosity is represented by the crenulation cleavage of F_2 folds. In mica-rich quartzite it mostly occurs as *discrete crenulation cleavage* cutting across S_1 S_3 cleavage is generally thicker (M-domain) and in quartz-rich pelitic gneisses it occurs as discrete *crenulation cleavage* as well as *smooth disjunctive cleavage* and the width of each cleavage domain varies between 4mm and 8 mm.

4.2.3. Lineations

Lineations constitute an important tool in this region for recognising probable mechanism of different episodes of folding. Four generations of lineations have been recognised. They are denoted as L_1, L_2, L_3 and L_4 **(Table 4.2)**. These lineations occur as intersection lineation (intersection of axial plane and form surface of folds), striping lineation, mesoscopic fold axis lineations, stretched pebbles and boudin lineations, mineral lineations. L_1 occurs both as intersection, striping and mineral lineations and are generally deformed. L_2 occurs as intersection lineations and mesoscopic fold axis lineations and they are less deformed by later foldings. L_3 and L_4 are hardly deformed and they usually occur as pucker axis and kink axis respectively.

4.3 SECTOR WISE DESCRIPTION

On the basis of outcrop pattern, availability of structural elements the area is divided into six sectors and the geometry of the folds are described sector wise: Sector-I- around Goidia-Barwarda, Sector II- around Wawadi, Sector III- around Luni, Sector IV- around Chhota Udepur, Sector V- around Longami, Sector VI- around Moti Sadli **(Fig.3.2)**.

Sector I- Goidia-Barwarda: The metasedimentaries in this sector occur as 2.5 km long and 750m wide arcuate ridge near Goidia and also seen in the low lying undulatory terrain in the east of Barwada within intrusive granite country **(Fig.3.2.1)** S_0 surfaces are only common in Goidia area within ferruginous quartzite and manganiferous quartzites and deformed conglomerates, represented by where compositional bands of variable thickness. Both $\mathbf{F_1}$ and $\mathbf{F_2}$ are recognisable at places and both are reclined in nature.

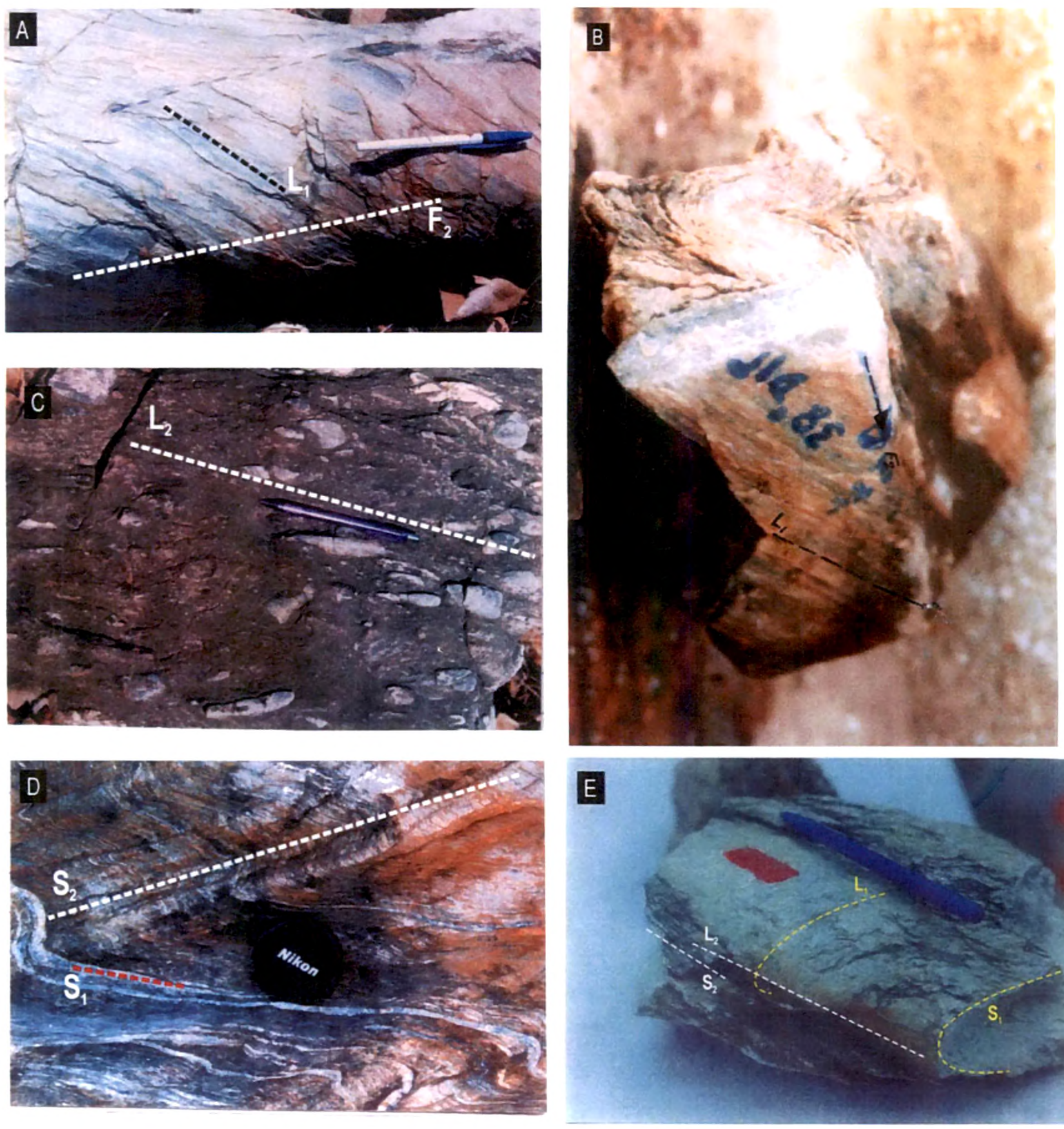

Plate 4.1.a) Early lineation (L_1)has rotated around the hinge of the later, Fold (F_2). F_2 having broad hinge, Goidia , b) Early lineation(L_1)has rotated around the hinge of the later, Fold (F_2) axis. F_2 having sharp hinge; c) Deformed conglomerate pebble shows strong elongation along F_2 near Goidia. D) "Z" shaped geometry exhibited by F_2 folds in the eastern slope of Goidia hill
E) Tight F_2 folds in kyanite schist near Wawadi.

F_1 folds occur only as rootless folds. In this sector the ferruginous quartzite bands occur within and micaceous quartzite and exhibit different wavelength of F_2 folds because of competency contrasts. The prominent folds are F_2 and have strongly developed crenulation cleavage as S_2. The early schistosity (S_1) is continuous and closed spaced. In general S_2 is southwesterly dipping. L_2 lineation shows an average plunge of 20° towards N60°W. The early lineation which are seen to have been rotated around F_2 hinges are recognised in the southwestern slope of Goidia hill (**Plate 4.1a and 4.1b**) as L_1 lineations in this area and are disposed with F_2 by an acute angle. The deformed conglomerate pebbles show a strong elongation along F_2 fold axes (**plate 4.1.c.**). In Goidia F_2 folds generally exhibits "*Z*" shaped geometry (**plate. 4.1.d.**) as seen in the eastern slope of Goidia hill. Here the S_2 crenulation is seen to have produced thick microlithons cutting across very closely spaced S_1. There are minor impacts of F_3 folds on such a quartzite-dominant terrain.

Sector II-Wawadi -Kasum: In Wawadi -Kasum area quartz-muscovite gneiss show distinct S_1 and S_2 surfaces as also recorded in sector 1. Unlike other places S_1 and S_2 intersect at acute angle (**Fig 4. a.**). S_2 crenulation cleavage in Wawadi area developed within quartz-rich muscovite-biotite schist, microlithons in crenulation cleavage are spaced 3 to 4 mm wide. In this sector F_1 occur as rootless folds in mesoscopic scale. Such folds are also seen in quartz veins, showing variable thickness, with a general thickening in the hinges. F_2 folds are having *S, Z,* as well as Σ shaped (**Fig 4 b, c, d.**) geometry. Here the F_3 occurs as low amplitude mesoscopic upright folds and steeply dipping F_3 fracture cleavage is prominent along the south-western slope of Wawadi hill. Variations of wavelengths of folds are noted within quartzite and co-folded mica schist (**Fig 4.b**). Just south of the village Wawadi F_2 -F_3 coaxial folds are recorded (**Fig 4.e.**). There are also N-S trending kink bands (related to F_4 folds) in this area, which are widely spaced (2 to 4 cm). Kyanite crystals of two generation (D_1 and D_2) are seen to have developed at places, where the elongated kyanite blades of different are high angels to each other.

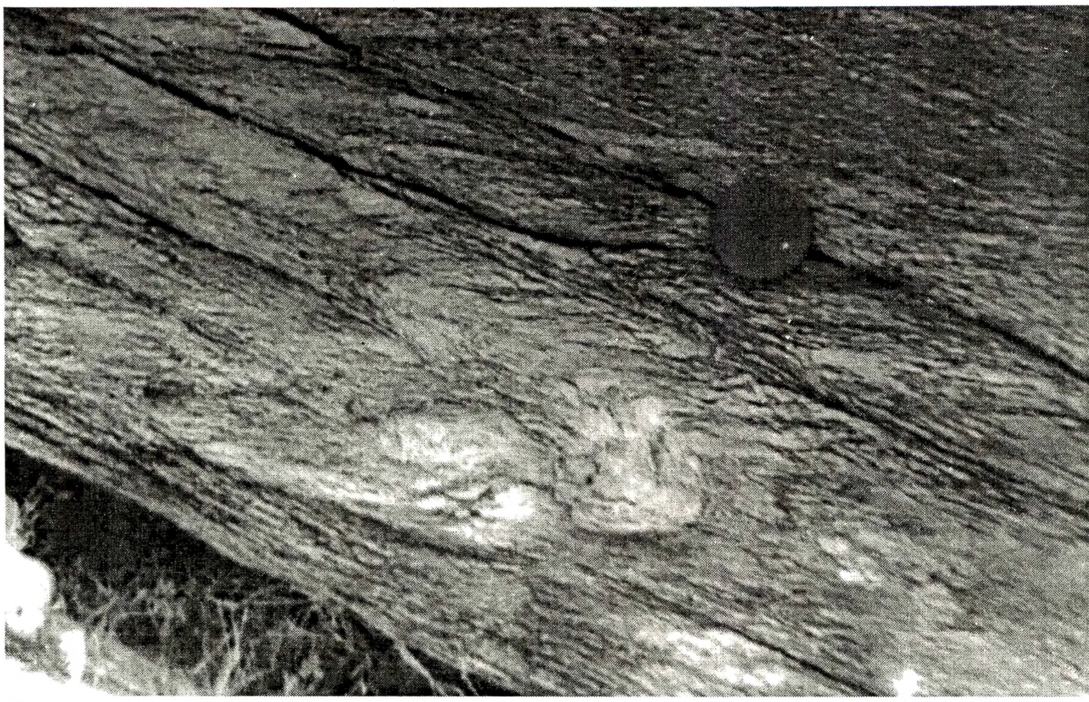

Fig 4.a S_2 crenulation cleavage in Wawadi area developed within quartz-rich muscovite-biotite schist, where S_2 is an acute angle with S_1

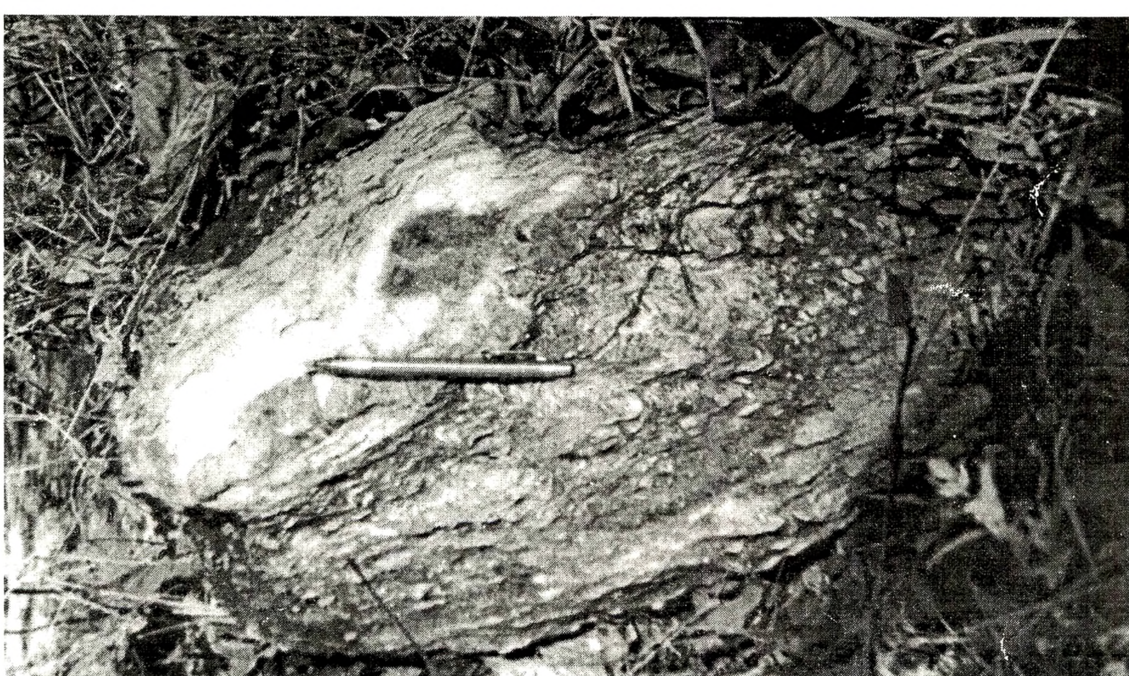

Fig 4.b. S-shaped F_2 folds. Variations of wavelengths of folds are noted within quartzite and co folded mica schist.

Fig.4.c. Z -shaped F_2 folds exhibited by quartz vein within mica schist near Wawadi.

Fig.4.d. Σ- shaped F_2 folds exhibited by quartz veins and micaceous quatzite near Wawadi

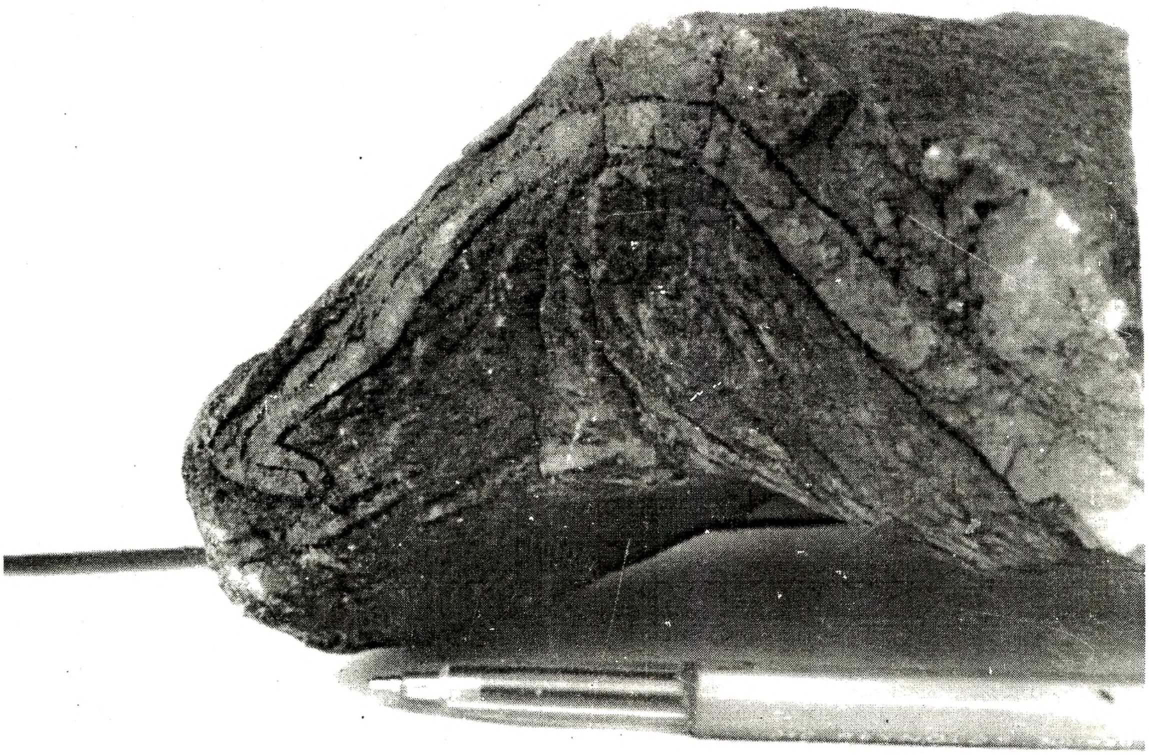

Fig. 4. e. F_2 -F_3 coaxial folds are recorded, south of Wawadi.

Sector III-Luni: In this sector both $\mathbf{F_1}$ and $\mathbf{F_2}$ folds are present in micaceous quartzite. Both the folds are tight isoclinal in nature and exhibit chevron geometry. Distinct $\mathbf{F_2}$ folds are preserved in micaceous quartzite in and are characterised by flattened limbs and thickened hinges. In this sector $\mathbf{F_2}$ folds are having ***Z*** shaped as well as Σ shaped geometry. **Z** shaped fold near Luni show sharp hinges within micaceous quartzite (**plate 4.2.a**), whereas Σ shaped folds are noted with quartzite, which too have sharp hinge(**Fig 4 f)**

Fig. 4. f. Σ shaped F_1 folds are noted with quartzite, which too have sharp hinge

The early L_1 lineations are disposed at a high angle around sharp F_2 hinges. The angle between F_1 fold axis (L_1) and F_2 fold axis (L_2) is maximum near Luni (80° to 90°, Fig.4.g). Impact of F_3 and F_4 folds is rare in this region and has hardly deformed the highly competent quartzites.

Sector IV - Chhota Udepur - Vagtaldungar: This sector comprises granite gneiss and intrusive granite. F_1 and F_2 folds, both reclined in nature are recognized within the sillimanite bearing schist and quartzite bands occurring in mesoscopic scale. Interference of these two folds is recorded near Vagtaldungar. Folded pegmatite vein (F_2) effected by shearing is also noted here (**plate 4.2.b**).Formation of pegmatite may be correlated with D_1.

Sector V -Longami: South of Longami within alternating leucocratic and melanocratic bands (parallel to S_2) of garnet -biotite- cordierite- sillimanite gneiss F_1 occurs as mesoscopic rootless folds (**plate 4.2.c**). At places distinct abutment of S_1 (discontinuous) against S_2 (dominantly penetrative) are recorded at Longami. The S_1 schistosity is folded by F_2 folds. S_2 is quite penetrative and places F_2 also occurs as mesoscopic rootless folds. The reclined F_2 hinges are seen prominently thickened. The folds are disharmonic in nature and die out within a short distance along successive layers. Both Σ shaped and S shaped mesoscopic F_2 folds are present in this area.

Fig 4. g. The angle between F_1 fold axis (L_1) and F_2 fold axis (L_2) is maximum near Luni (80° to 90°)

Sector VI-Moti Sadli: In this sector sillimanite and garnet bearing biotite gneiss show various deformational structures. S_1 schistosity is not easily recognisable in this sector, except in areas where biotite schist contain thin bands of quartzite. F_2 folds are reclined in nature and mainly plunge towards east to southeast. Effect of F_3 on F_2 is well recorded in many a places in the eastern slope of the Moti Sadli Hill and also to the west of the village. One of the exposed limb of F_3 fold is seen to have affected F_2 foliation producing upright fold, in the eastern slope of Moti Sadli Hill **(plate 4.2.d)**

Morphology and nature of the folds

The morphology of F_1 and F_2 are shown in the following tables (Table 4.3. a and 4.3.b.). data indicates that the folds have large amplitudes/ wavelength ratios and having considerable thickening of hinge. However, F_2 developed in pelitic schists in particular, exhibit much greater thickening of hinge.

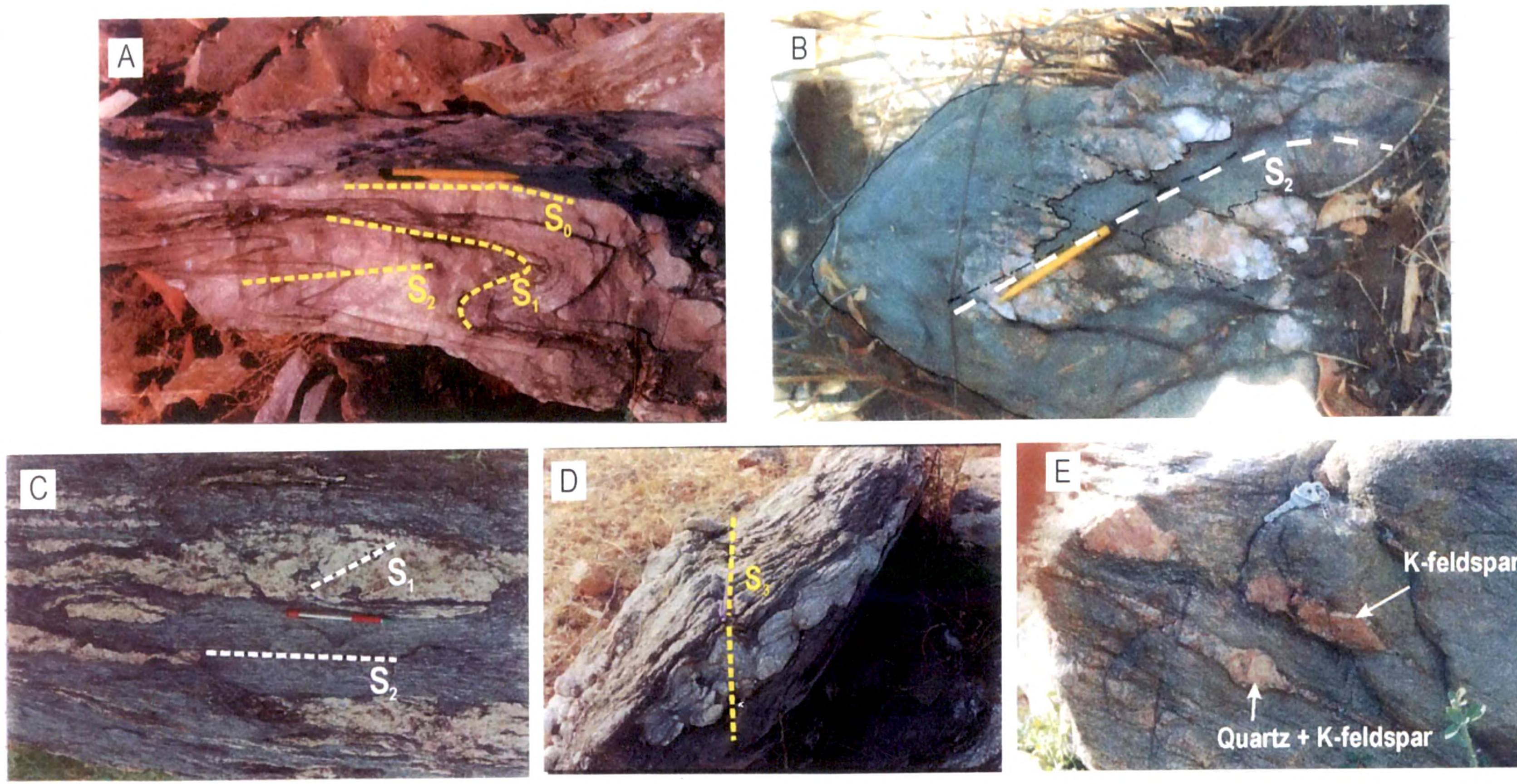

Plate 4.2 a. *Z* shaped geometry of F_2 fold near Luni; b. Folded pegmatite vein (F_2) effected by shearing is noted, east of Chhota Udepur; c South of Longami within alternating leucocratic and melanocratic bands (parallel to S_2) of garnet -biotite- cordierite- sillimanite gneiss F_1 occurs as mesoscopic rootless folds; d. One of the exposed limb of F_3 fold is seen to have affected F_2 foliation producing upright fold, in the eastern slope of Moti Sadli Hill; e. Brittle deformation in k-feldspar vein and ductile deformation in quartz + k-feldspar veins

Table 4.3.1 Table showing deformational style of Precambrians of Southern Rajasthan and Gujarat. Various episodes of folding in (A) the main Aravalli Fold Belt (Rajasthan) and (B) In Chhota Udepur region, Gujarat.

*A (after Sychanthavong, 1990)				*B Present Observation	
Major episodes of foldings	Naha and Halyburton; 1974, Naha et al ,1984	Sychanthavong and Merh 1981	Morphology of various folds in general	Pre-Champaner Gneisses	Champaner Group
Pre-Delhi folding (around 2500Ma)	AF_1	·	Isoclinal reclined folds (E-W)	F_1 Reclined folds plunge mainly north and south	--
First Dehi Foldings (1600Ma to 1400Ma)	AF_2	DF_1	Isoclinal recumbent folds with NNW-SSE axial trace	F_2 Reclined folds , plunge mainly east and west	--
Second Delhi Foldings (1400 Ma-700Ma)	AF_3 AF_4	DF_2 DF_3	Doubly plunging upright folds NNE-SSW	F_3 E-W trending upright folds coaxial with F_2	F_3 E-W trending upright fold, first deformation in Champaners
Third Folding (1900 Ma-500Ma)		·	Northerly overturned in southern parts, doubly plunging domes in the central and northern part.	F_4 Upright warps with N-S trending kink bands.	F_4 N-S trending warps with kink bands

Table 4.3.2 Morphology of F_1 folds in different localities

Places *Sector*	Goidia Sector I	Luni Sector II	Wawadi Sector III	Chhota Udepur Sector IV
Lithology	Quartzite	Quartzite	Quartzite	Quartzite
Average hinge/limb thickness ratio	1.33	1.2	1.3	1,5
Amplitude/ wavelength ratio	-	2.5	2.25	-

Table 4.3.3. Morphology of F_2 folds in different localities

Places *Sector*	Wawadi Sector II	Goidia Sector I	Luni Sector III	Chhota Udepur Sector IV	Longami Sector V	Moti Sadli Sector VI
Lithology	Vein quartz	Quartzite	Quartzite	Granite gneiss	Sill- garnet- biotite- gneiss	Sill-garnet- biotite- gneiss
Average hinge/ limb thickness ratio	1.8	1.33	1.25	1.5	2.2	2.1
Amplitude/ wavelength ratio	2.75	2.25	2.5	2.2	2.5	Could not be determined

4.4 STRUCTURAL ANALYSES

4.4.1 Introduction

Structural analyses was carried out using Smidt's equal area stereographic net. Both foliation (S_1, S_2 and S_3) and lineation (L_1 L_2, L_3 and L_4) data were used which are shown in **Figures. 4.2.1** to **4.2.7**. On the basis of constancy of L_2 lineations the area have been divided into six isolated sectors: 1) *Sector I*- Goidia –Barwada; 2) *Sector II*- Wawadi-Kasum; 3) *Sector III*- Luni; 4) *Sector IV* -Chhota Udepur- Vagtaldungar; 5) *Sector V*-Longami and 6) *Sector VI*- Moti Sadli.

By and large it is observed that the poles of S_1 planes are scattered (Fig. **4.2.5**) due to the effect of F_2 reclined folds as well as F_3 folds. Limited S_1 data are only recorded within these five sectors. S_2 poles are plotted for whole of the regions(**Fig 4.2.5**) which include data from the isolated five selected sectors and from gneissic country rocks outside the sectors. Although S_1 is low dipping around the hinges they are sub-vertical. Similarly the L_1 lineations are spread due later folding, however, they are generally southerly or northerly plunging. From the study of linear and planar elements it is inferred that L_2 and S_2 show a little variation in orientation within these individual sectors. A fairly wide spread of L_2 was noticed due to the effect of F_3 folding. It is also seen that these lineations neither fall in a great circle nor in a small circle, which is one of the evidences that the F_3 folding was of buckle folding nature, with post buckle flattening. As the amplitude / wavelength ratios of F_3 folds are very low, local impact of F_3 folding is much less in this terrain and is clearly reflected in the equal area projection. The S_2 poles in individual sector do not show much variation in orientation, but when they are compared regionally they show scatter in great circle indicating a regional effect of F_3 folding. This analysis may also be corroborated with the study of the structural trends in map where presence of macroscopic F_3 folds is recorded on a regional scale.

Figure 4.2.1 a

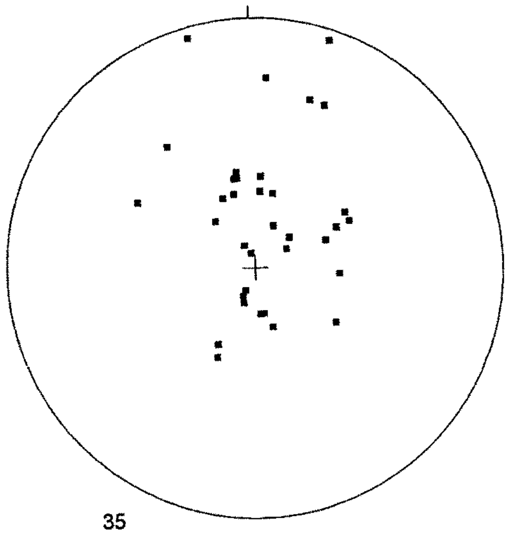

Sector I

35

Number of data

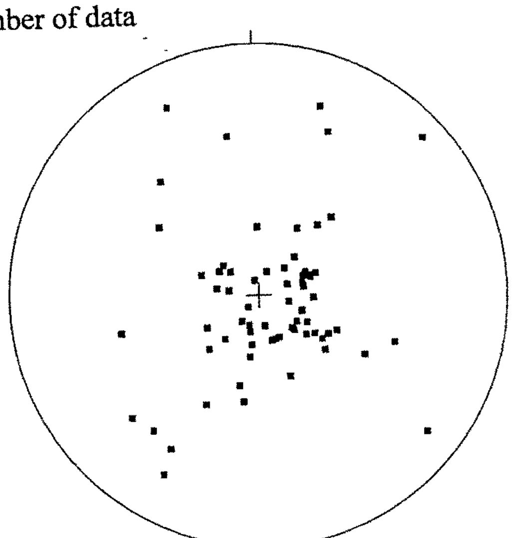

Sector-II

70

Number of data

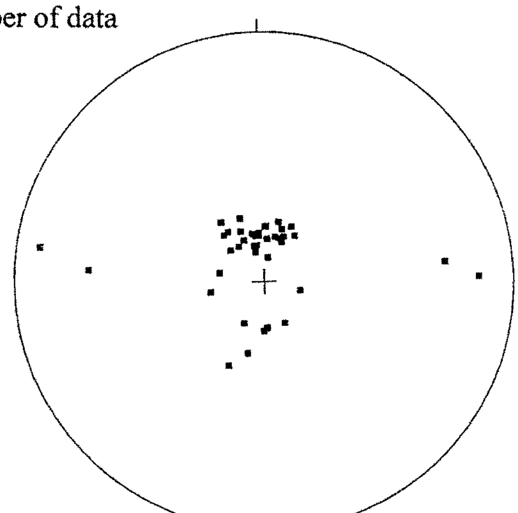

Sector-III

42

Number of data

S_1 Poles plotted for different sectors

Figure 4.2.1.b

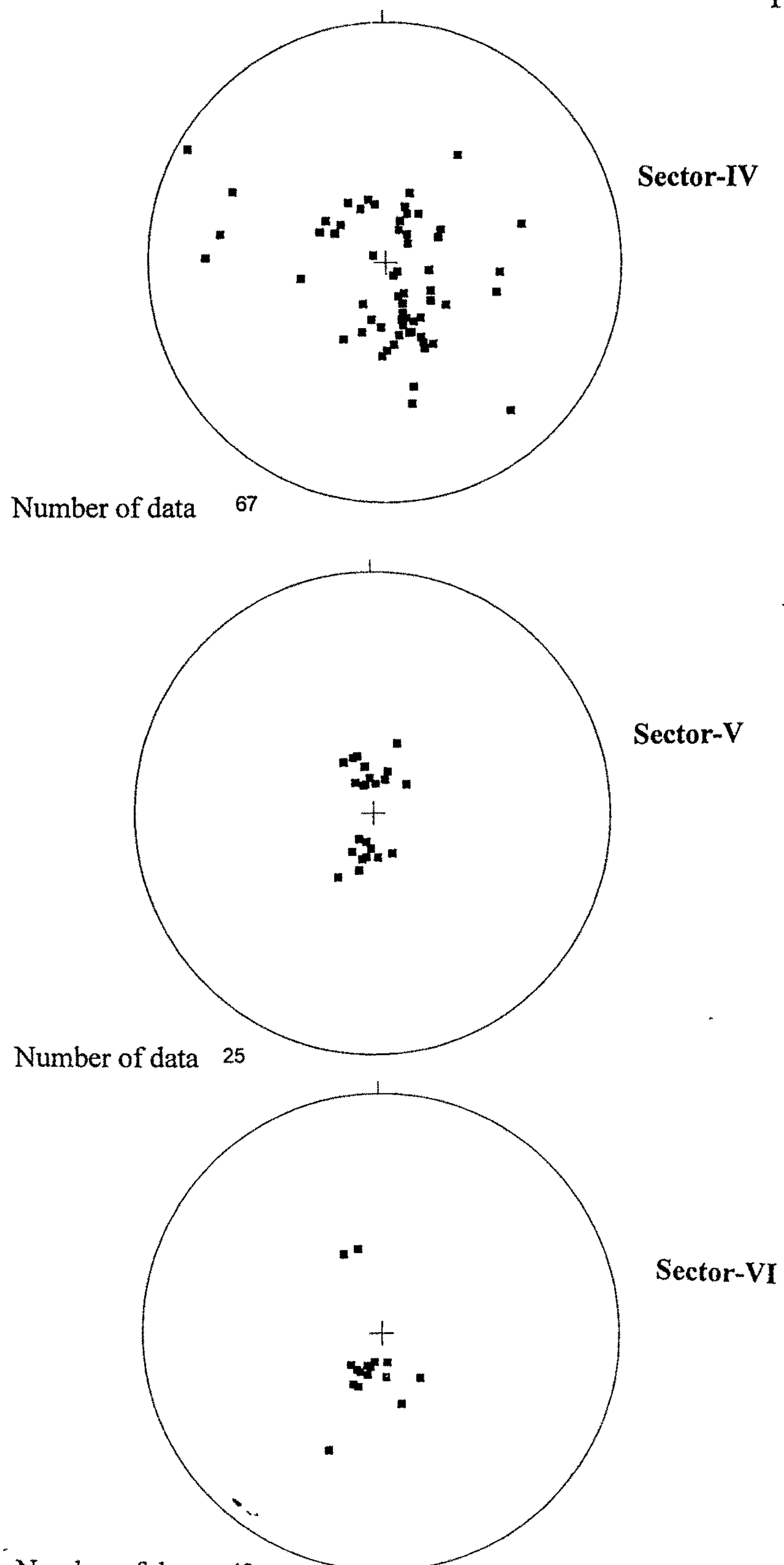

. S_1 Poles plotted for different sectors

Figure 4.2.2.a

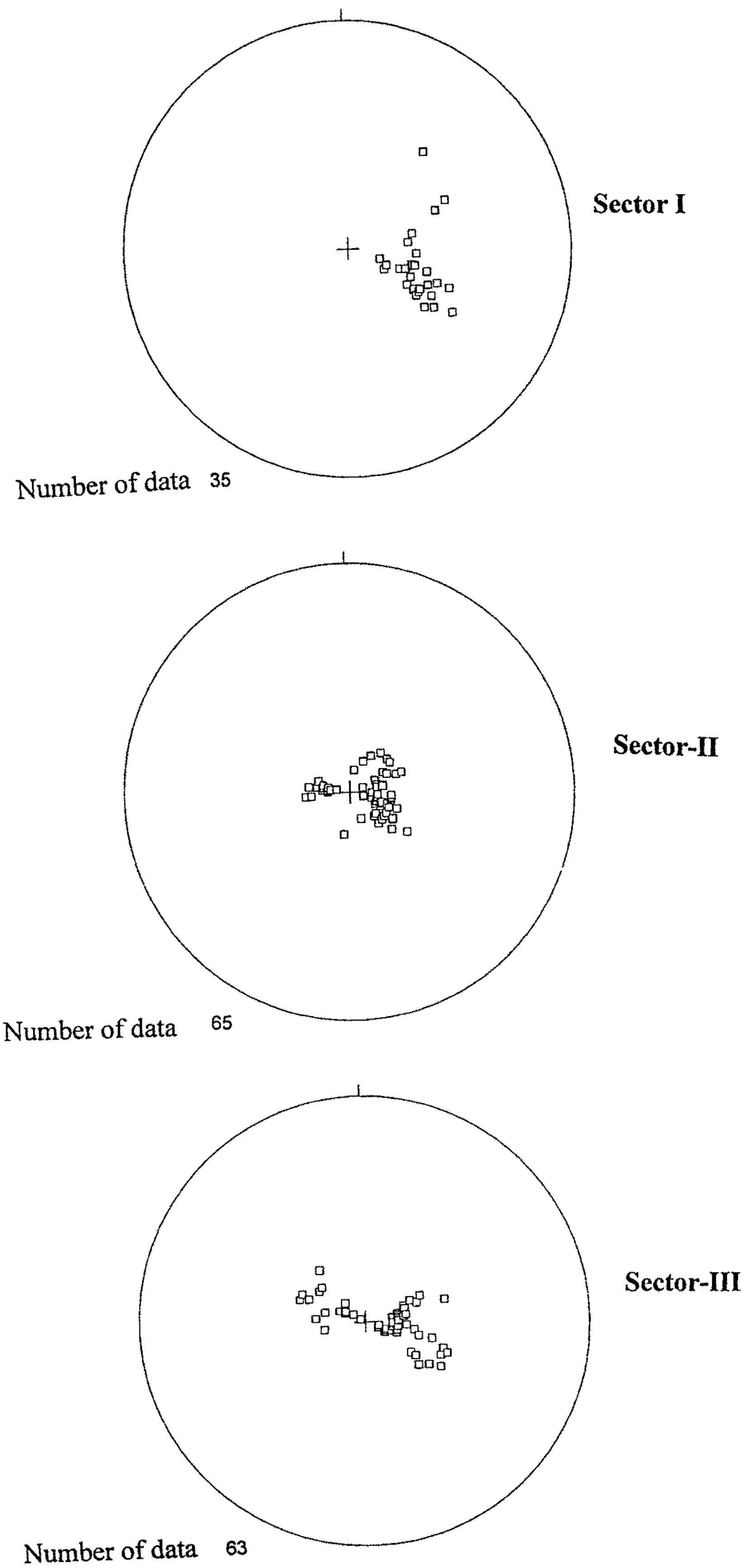

S_2 Poles plotted for different sectors.

Figure 4.2.2. b

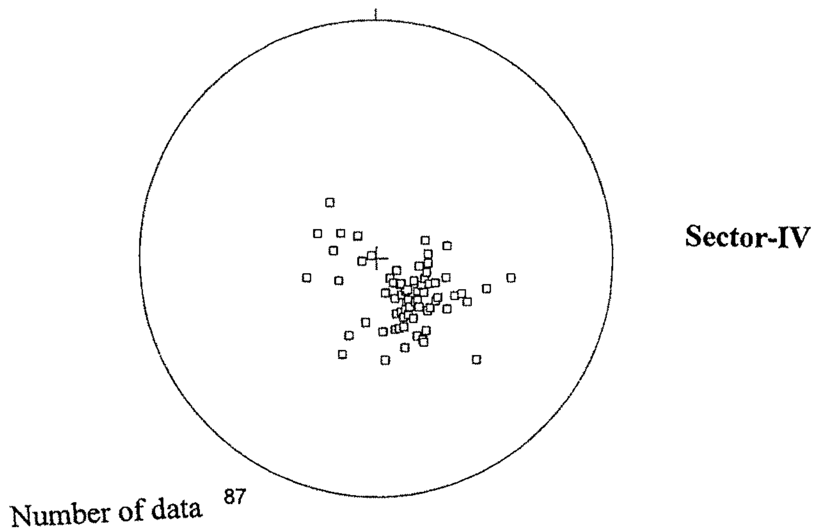

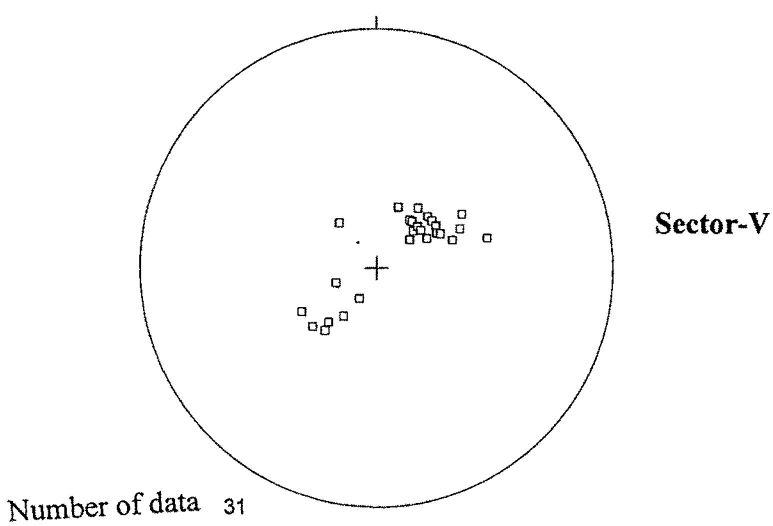

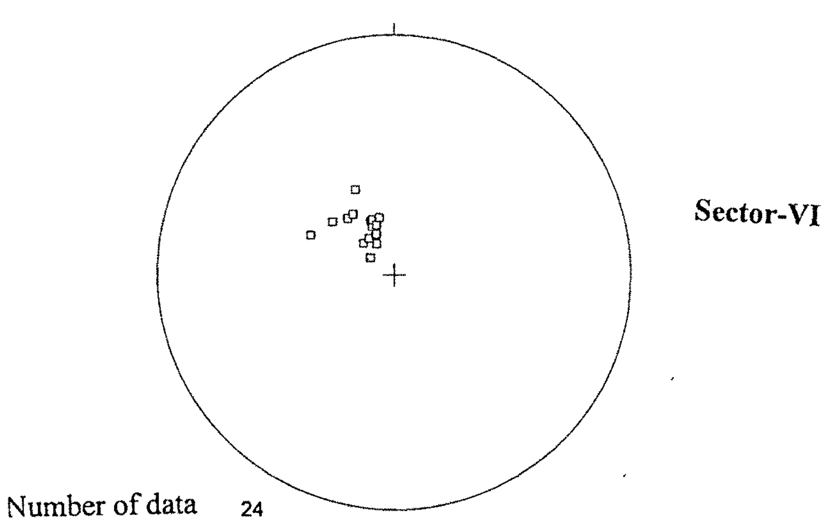

S_2 Poles plotted for different sectors.

Fig 4.2.3a

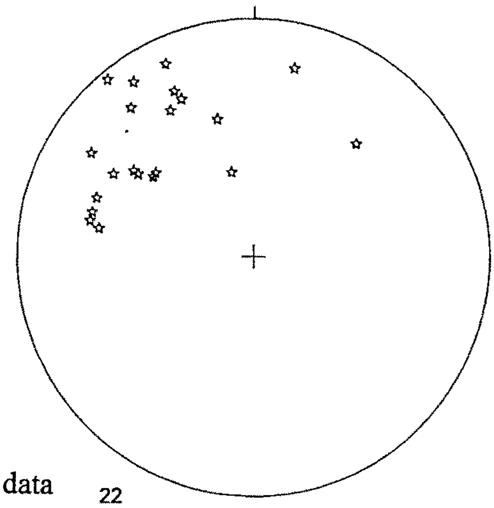

Sector I

Number of data 22

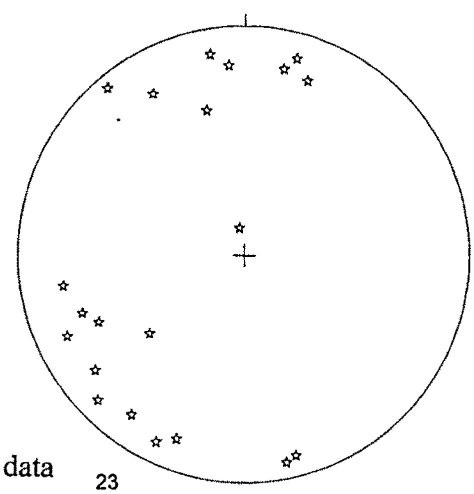

Sector-II

Number of data 23

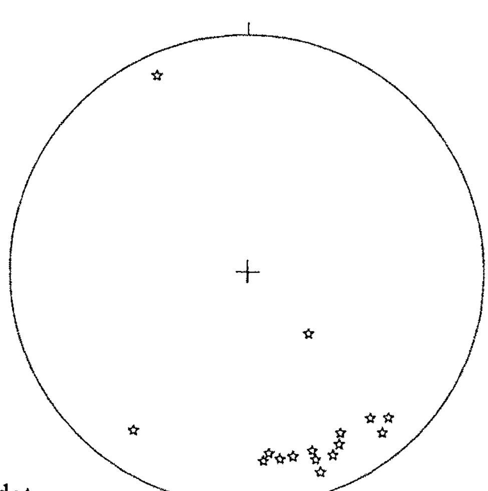

Sector-III

Number of data 16

Plunge of L_1 lineations for different sectors

Fig 4.2.3b

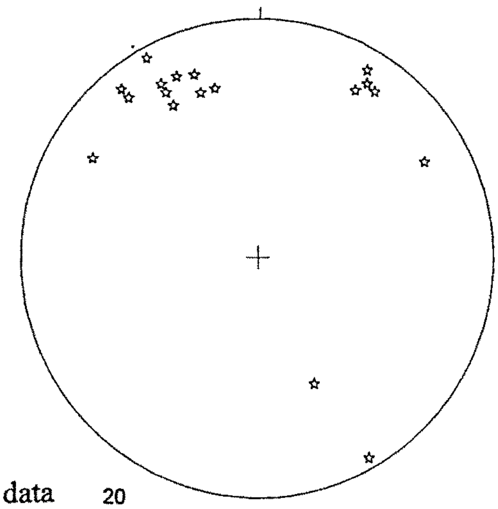

Sector IV

Number of data 20

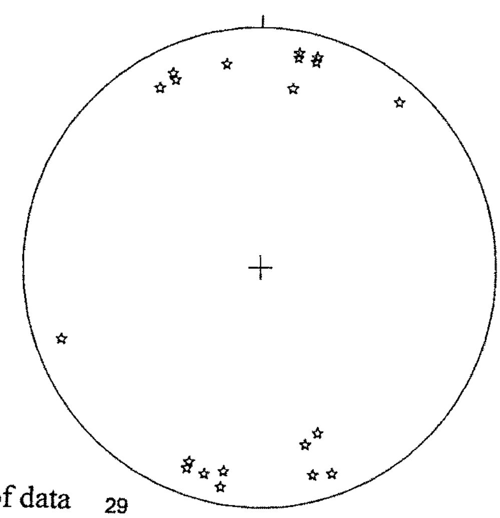

Sector V

Number of data 29

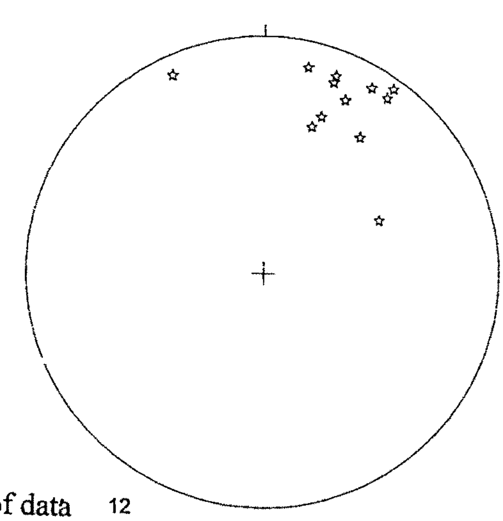

Sector VI

Number of data 12

Plunge of L_1 lineations for different sectors

Fig 4.2.4a

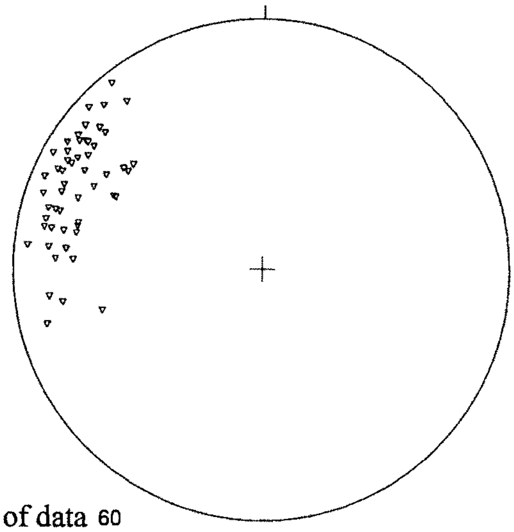

Sector I

Number of data 60

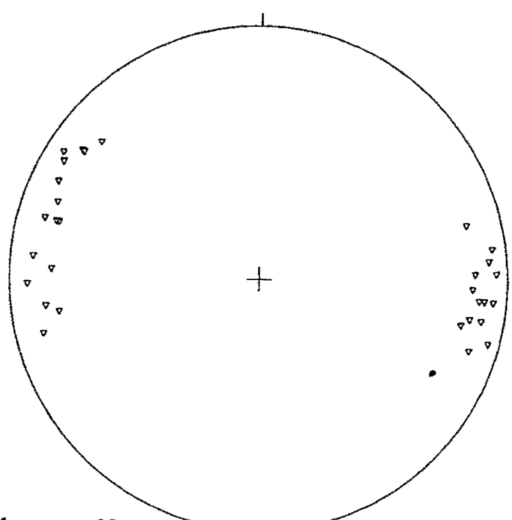

Sector-II

Number of data 30

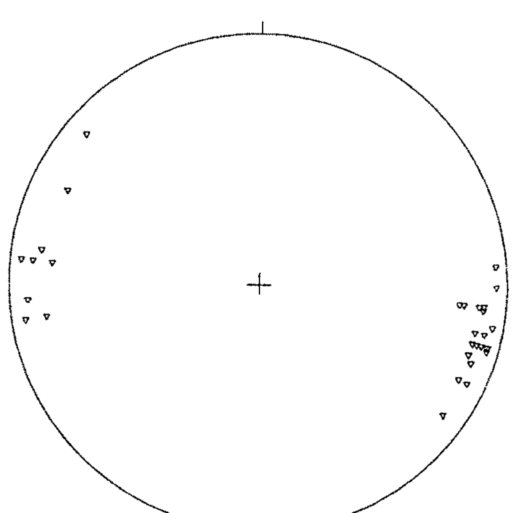

Sector-III

Number of data 36

Plunge of L_2lineations for different sectors

Fig 4.2.4.b

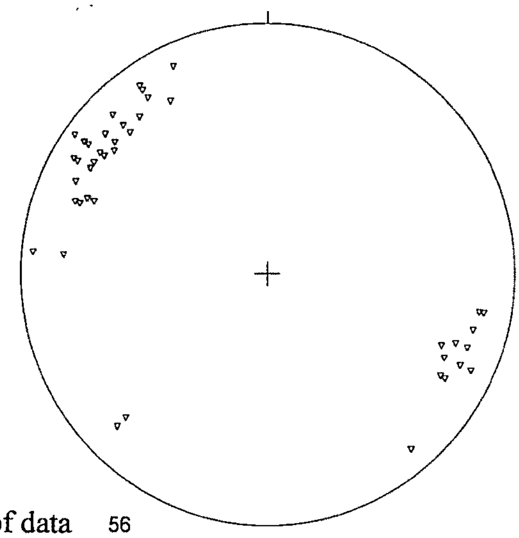

Sector IV

Number of data 56

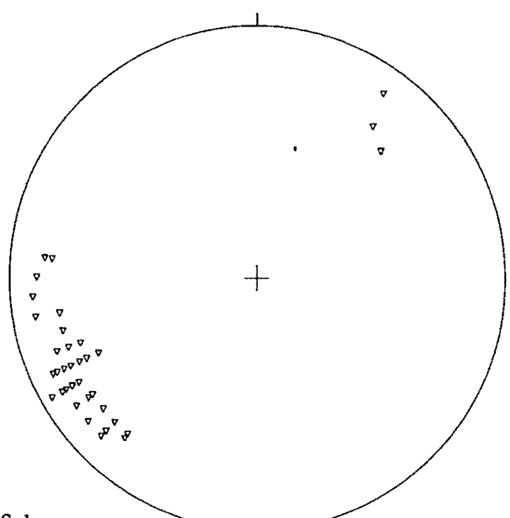

Sector V

Number of data 54

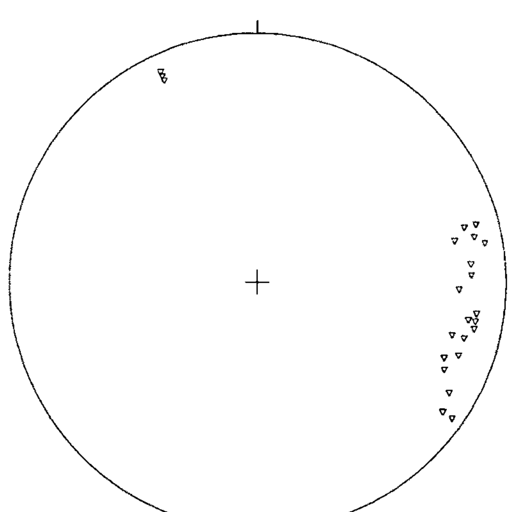

Sector VI

Number of data 32

Plunge of L_2 lineation for different sectors

Fig 4.2.5

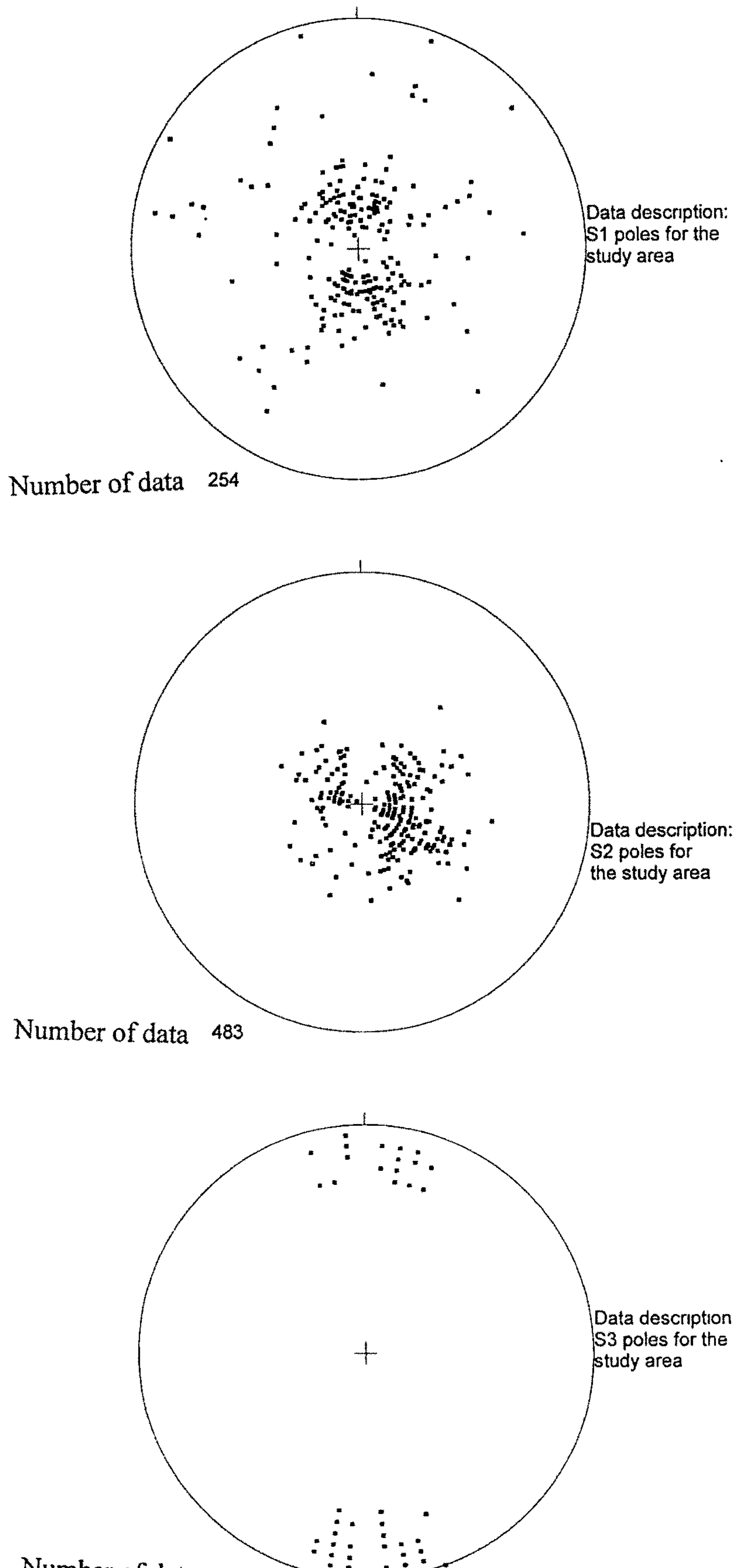

S_1, S_2 and S_3 poles plotted for the study area

Fig 4.2.6

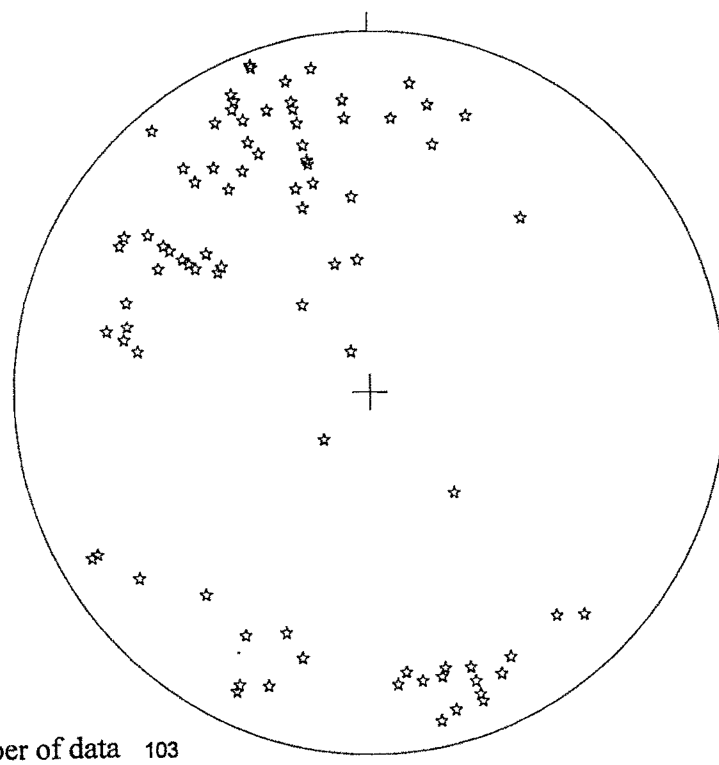

Plunge of L_1 lineations

Number of data 103

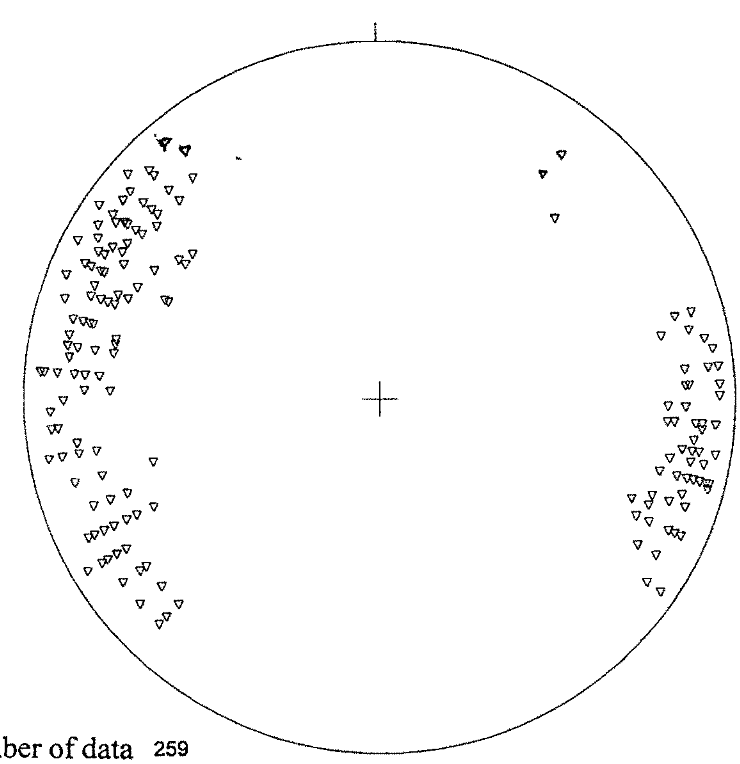

Plunge of L_2 lineations

Number of data 259

Plunge of L_1 and L_2 lineations for the study area

Fig 4.2.6a

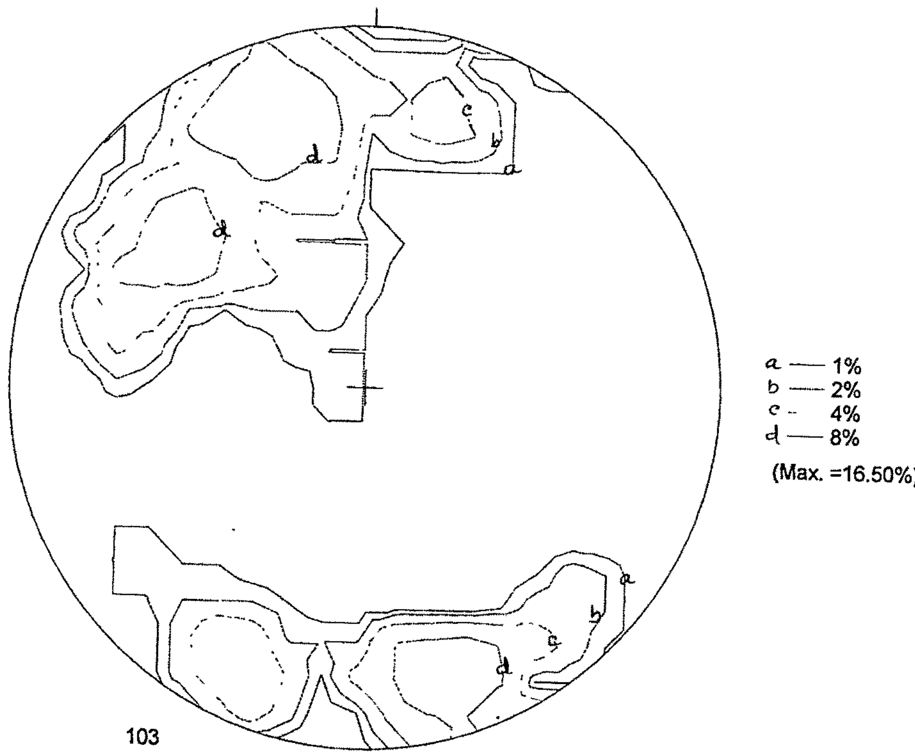

Contours showing concentration of L_1 lineation plunge

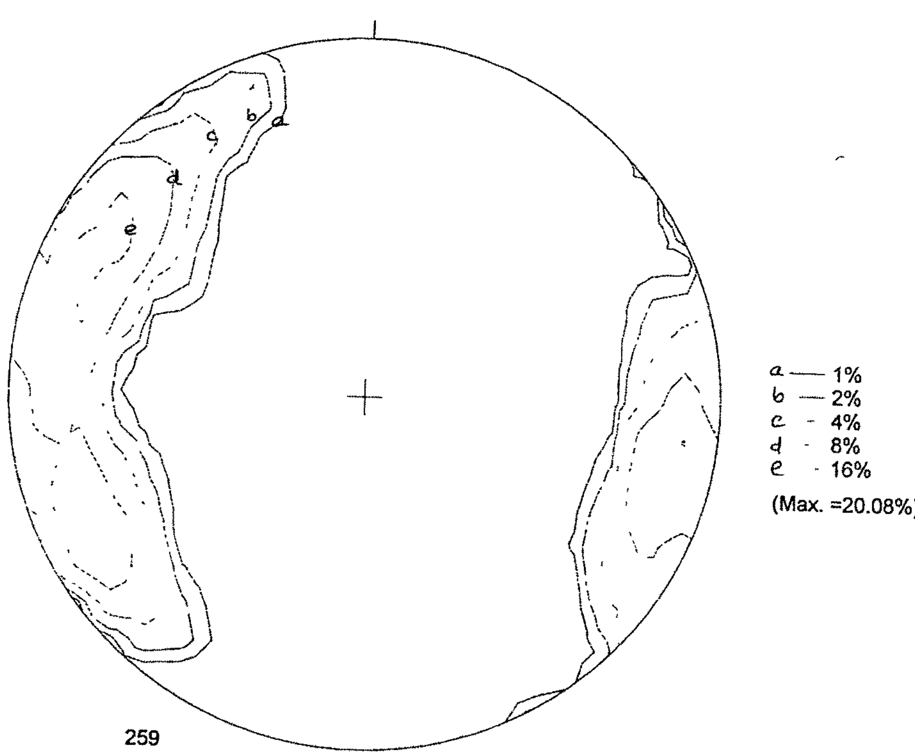

Contours showing concentration of L_2 lineation plunge

Fig 4.2.7

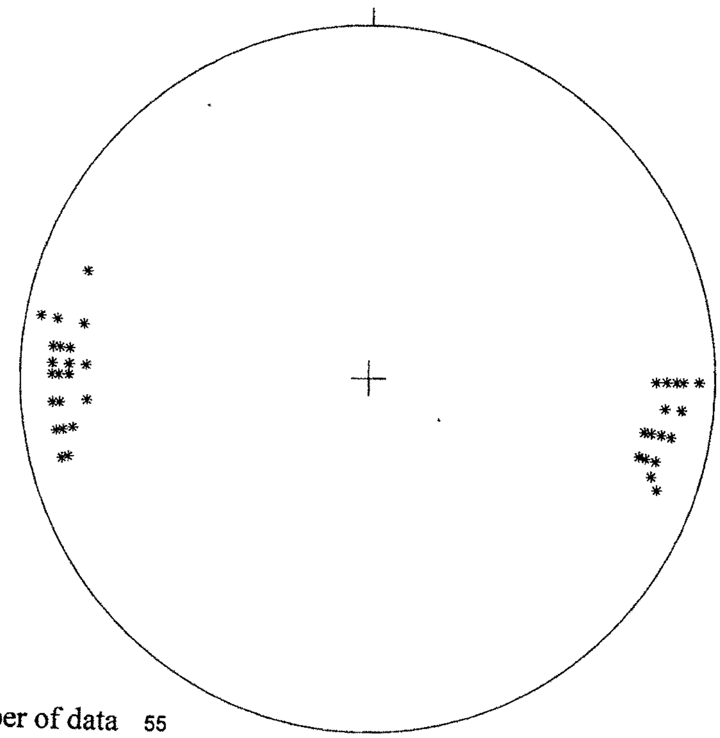

Number of data 55

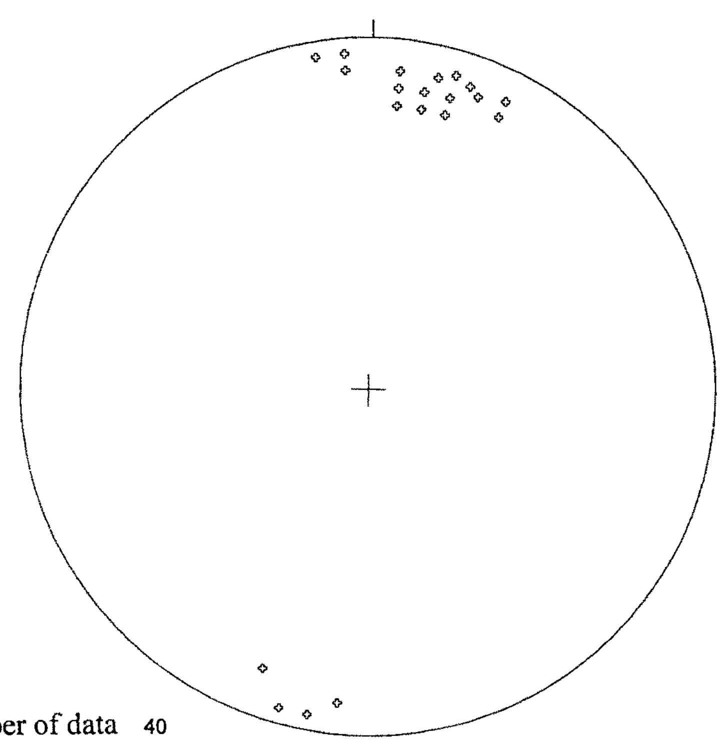

Number of data 40

Plunge of L_3 and L_4 lineations for the study area

4.4.2. Relation of deformed lineations to the genesis of folding

Three distinct types of deformed lineations have been recorded in this area (**Fig 4.3.**). Following the classification of Ghosh and Chatterjee (1986), these are considered as type '2a', type '4' and one unrollable type. The first two types have been develop in restricted conditions such as in the case of flexural slip folding followed by homogeneous flattening. However, the third type, which is *unrollable type*, recorded near Luni Dam the L_1 lineation is unrollable around F_2 hinges. This may develop in the case of pure flexural slip folding of non-coaxial deformation. Similarly type '2a' and '2b' deformed lineation pattern around $\mathbf{F_3}$ hinges where $\mathbf{F_2}$ and $\mathbf{F_3}$ are mutually coaxial have also been recorded (evidenced by interference pattern).

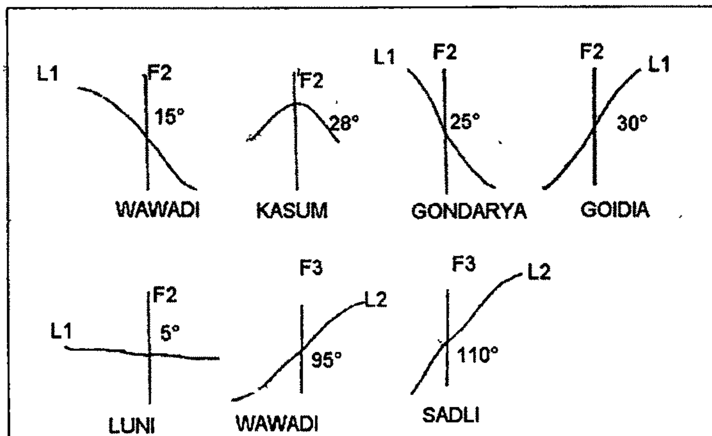

Patterns of L1 and L2 lineations around single F2 and F3 fold axes respectively. Figures shown in degrees are interlimb angles

Fig 4.3 Patterns if L1 and L2 lineations around single F2 and F3 fold axes respectively.

According to Mukhopadhyay and Ghosh (1980), dissimilar lineation pattern in an area may develop due to initial inhomogeneous strain in rocks of different competency or nonsynchronous development of mesoscopic F_2 folds in different parts of larger folds. Evidence in favour of the first statement clearly holds good as in Luni area pure flexural slip folding with negligible post buckle homogeneous strain (indicated by unrollable lineation) is exhibited by competent layer (quartzite) and other two types where probably post buckle homogeneous flattening was dominant are recorded within pelitic schist around Wawadi and Goidia. However, relation between $\mathbf{F_2}$ hinges and $\mathbf{L_1}$ lineations clearly indicates that $\mathbf{D_2}$ is non-coaxial deformation. Distribution pattern of $\mathbf{L_2}$ lineation on stereographic projection and morphology of the $\mathbf{F_3}$ fold indicate that $\mathbf{D_3}$ is buckle fold with post buckle flattening. This is also supported by the disharmonic nature of the folds and relation between the competent and incompetent layer in mesoscopic folds wherein incompetent layers of mica schist show much higher wavelength than the competent quartzite layer, which is an example of buckle folding.

4.4.3 Boudin chronology

There are two distinct generation of 'boudins'/ 'pinch and swell structures' recorded in the study area. 1) Related to $\mathbf{F_1}$ folding event or pre $\mathbf{F_2}$ folding event ; these boudins do not show congruous relationship with the $\mathbf{F_2}$ folds as in some cases the boudins are thicker in the limbs and thinner in the hinge. 2) Boudins and pinch and swell structures related to $\mathbf{F_2}$ folding event as recorded near Wawadi (**Fig.4.j**) and Goidia (**Fig.4.i.**) show thickening in the hinge zone with incipient boudinisation accompanied by minor folding whereas in the limb region they are of $\mathbf{F_2}$ folds and they are well developed and thickness (measured perpendicular to the $\mathbf{S_1}$ surface) is less. No boudin is seen to have formed during $\mathbf{F_3}$ folding. The boudins related to $\mathbf{F_2}$ folding, mostly show pull-apart structure, which are the result of pure shear (longitudinal strain). These boudins show rectangular as well as elliptical outline. A few boudins recorded near Chhota Udepur show imprints of local shearing (simple shear) which post dates pure shear. Here the boudins are occasionally rhombic. Two subparallel quartz-rich and feldspar-rich veins in Orsong river section of Chhota Udepur show pinch and swell/boudin structure respectively.

(**Plate 4.2**.E). In Koiwav and Goidia area quartz veins are extremely boudinased during F_2 folding event and the longest axes of boudins are sub parallel to the F_2 fold axes (Plate **4.1.c**).

4.4.4. Strain analyses

Strain analyses of the quartz veins occurring in the form of boudins and pebbles have been carried out for Pre-Champaner gneisses and Champaner Group separately. The longest axis, intermediate axis and shortest axis of the deformed boudins and pebbles measured for Pre- Champaner Gneisses are tabulated in **Table 4.4.1**. for analyzing in Flinn's diagram(**Fig. 4.4.1** and **4.4.2**).

Fig. 4.i. Pinch and swell structure near Wawadi

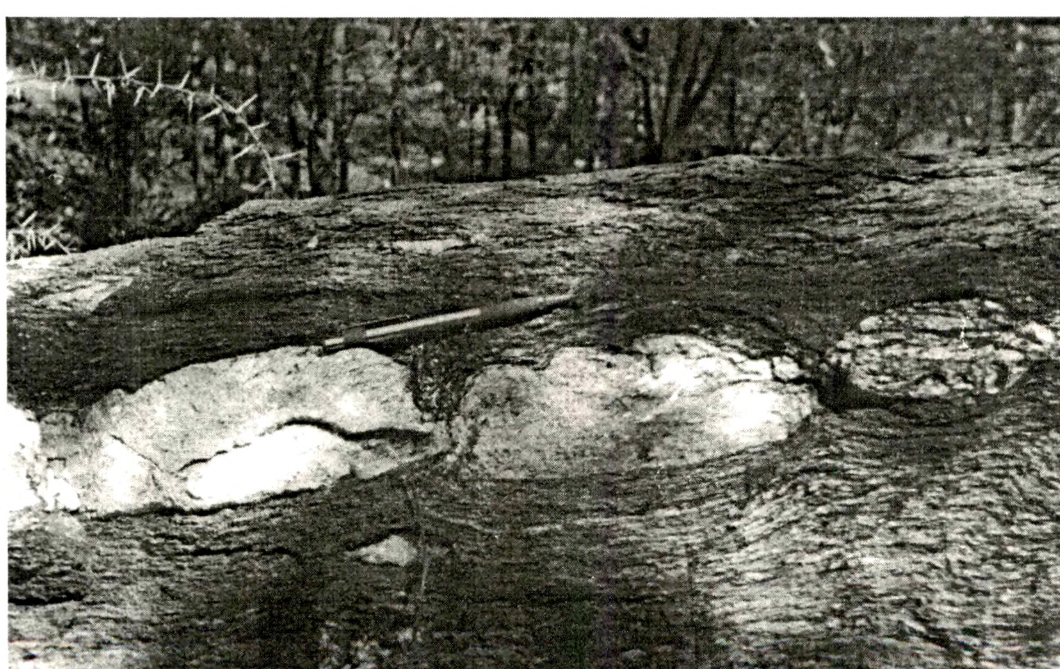

Fig 4.j. Rectangular boudin near Goidia

Table 4.4.1 Table showing shape and size of vein quartz boudins / quartzite/ magnetite quartzite pebbles in Pre- Champaner Gneiss

Number of observation	Length of boudin parallel to foliation and along F_2 fold axes); in cm. '*b*' longest axis	Length of boudin parallel to foliation and across F_2 fold axes; in cm. '*a*' Intermediate axis	Length of boudin perpendicular to foliation: in cm. '*c*' shortest axis	Intermediate/ shortest ('*X*' axis in Flinn's diagram)	Longest / intermediate ('Y' axis in Flinn's diagram)
1	18	6.5	3	2.16	2.76
2	12	4	2	2	3
3	14	6	4	1.55	2.33
4	19	7	3	2.33	2.71
5	14	5	2	2.5	2.8
6	11	6	2	3	1.83
7	20	8.5	3	2.83	2.35
8	14	5	2	2.5 .	2.8
9	22	6.5	3.5	1.85	3.35
10	21	7	2	3.5	3
11	15.5	5.5	3	1.83	2.81
12	19	6	4	1.5	3.16
13	18	5	2.5	2	3.6
14	18	6	3.5	1.71	3
15	14	5	2	2.5	2.8
16	16.5	8	5	1.6	2.06
17	11	4	2	2	2.75
18	21	12	6	2	1.75
19	15	7	3	2.3	2.2
20	14	6	3	2	2.33
21	14.5	5	2	2.5	2.85
22	15.5	6	2.5	2.4	3.58
23	12.5	5	2.5	2.4	2.5
24	5.2	2.1	1.9	1.25	2.5
25	12	5	3	1.75	2.6
26	6.5	2.5	1.5	1.65	2.6
27	8	3.5	2	1.75	2.2
28	8	3.5	2	1.75	2.2
29	6.5	2 5	1.1	2.5	2.75
30	21	10	5.5	1.82	2.1
31	20	7.5	3.5	2.33	2.65

The longest axes of boudins are generally conforming to F_2 axes in Goidia, Koiwav and Wawadi. Similarly the deformed pebbles of the conglomerate of central part of Goidia hill show a tendency to be aligned parallel to F_2 axes.

Considering the fact that the area has been dominantly affected by pure shear, strain analyses of the pebbles and boudinaged vein quartz show a general constrictional strain ellipsoid when analysed by Flinn's plot. The value of **Y** (ratio of longest axis / intermediate axis) varies from 1.75 to 3.58, indicating a fairly high degree of elongation and the value of **X** (intermediate axis/ shortest axis) vary from 1.25 to 3.5 indicating a variable degree of flattening. However Flinn's plot indicate an overall elongation of structural elements.

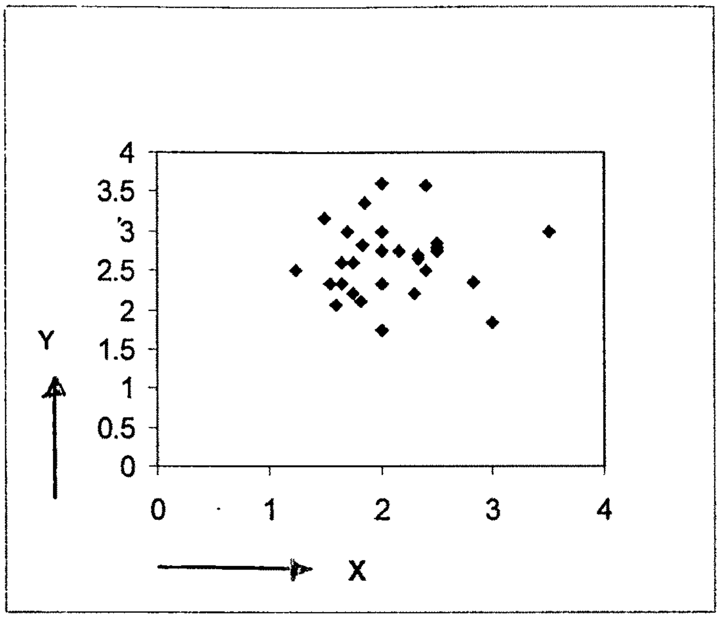

Fig. 4.4.1. Flinn's plot for strain analysis in quartz boudin and pebbles of Pre-Champaner Gneiss.

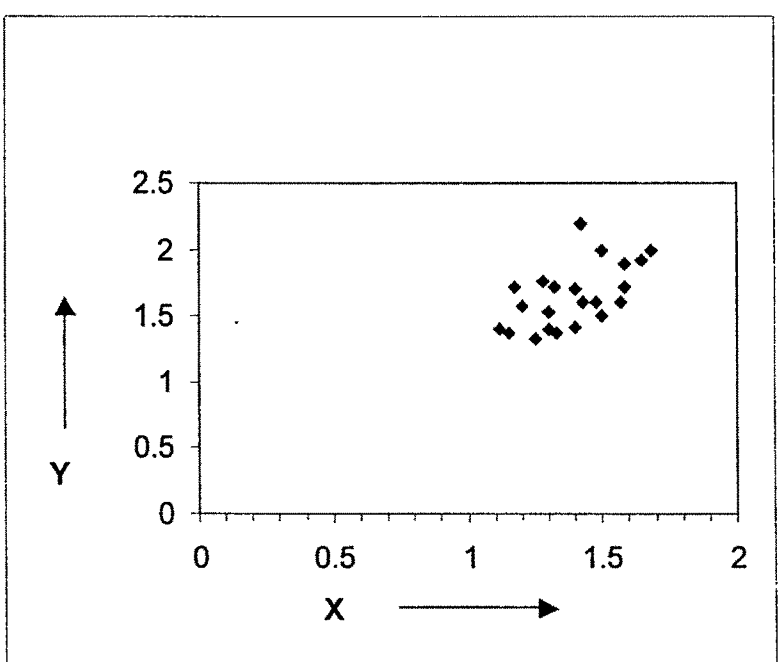

Fig. 4.4.2. Flinn's plot for strain analysis in quartzite pebbles in Champaner Group.

Quartzite pebbles of the Middle Champaner conglomerates also show a general constrictional strain effect on the terrain (**Table 4.4.2**). However, the degree of strain is less than those of the Pre-Champaner Gneiss boudins and pebbles. This is because of the fact that Champaner Group was not subjected to early two folding events ($\mathbf{F_1}$ and $\mathbf{F_2}$).

Table. 4.4.2 Shapes and sizes of quartzite/ magnetite quartzite pebbles in the conglomerate horizon of Middle Champaner Subgroup

Number of observation	Longest axis In cm	Intermediate axis In cm	Shortest axis In cm	Longest / inter-mediate axis	Intermediate/ Shortest axis
1	6	4.5	3.5	1.33	1.25
2	6	3	2	2	1.5
3	24	14	12	1.72	1.17
4	11	7	5	1.42	1.4
5	12	6	4	2	1.5
6	11	5	3.5	2.2	1.42
7	9	6	4	1.5	1.5
8	7	5	4.5	1.4	1.12
9	23	12	7.5	1.92	1.65
10	16	9	7	1.77	1.28
11	12	7	5	1.7	1.4
12	10.5	5.5	3.5	1.9	1.58
13	8	5	3.5	1.6	1.43
14	9	6.5	5	1.53	1.3
15	6	3.5	2.5	1.7	1.40
16	7	4	3	1.72	1.32
17	10.5	6.5	4.5	1.6	1.48
18	9	5.5	3.5	1.6	1.57
19	5.5	4	3.5	1.37	1.15
20	9.5	6	5	1.58	1.2
21	12	7	4.5	1.72	1.58
22	15	7.5	4.5	2	1.68
23	11	8	6	1.37	1.33
24	12	8.5	6.5	1.4	1.3

4.5. REGIONAL STRUCTURE BASED ON GEOPHYSICAL DATA

Geophysical data (Bouguer anomaly map, **Fig 4.5**) suggest that the Pre-Champaner Gneisses are strikingly different from Godhra granite and they have geophysical characteristics similar to a basement rock. While a ~ -30 mgl is recorded over Pre-Champaner Gneiss (designated as **X** in Fig.4.5) a lower value of ~-42 mgl is recorded over Godhra Granite (**Y** in **Fig. 4.5**). These two units are separated by ENE-WSW trending fault (designated as **F1** in **Fig 4.5**). Another fault oriented in WNW-ESE direction (**F2** in Fig.4.5) brings Godhra Granite (**Y** in **Fig. 4.5**) against Lunavada Group(**Z** in **Fig.4.5**).

Bouguer Gravity

Chhota Udepur Area, Eastern Gujarat

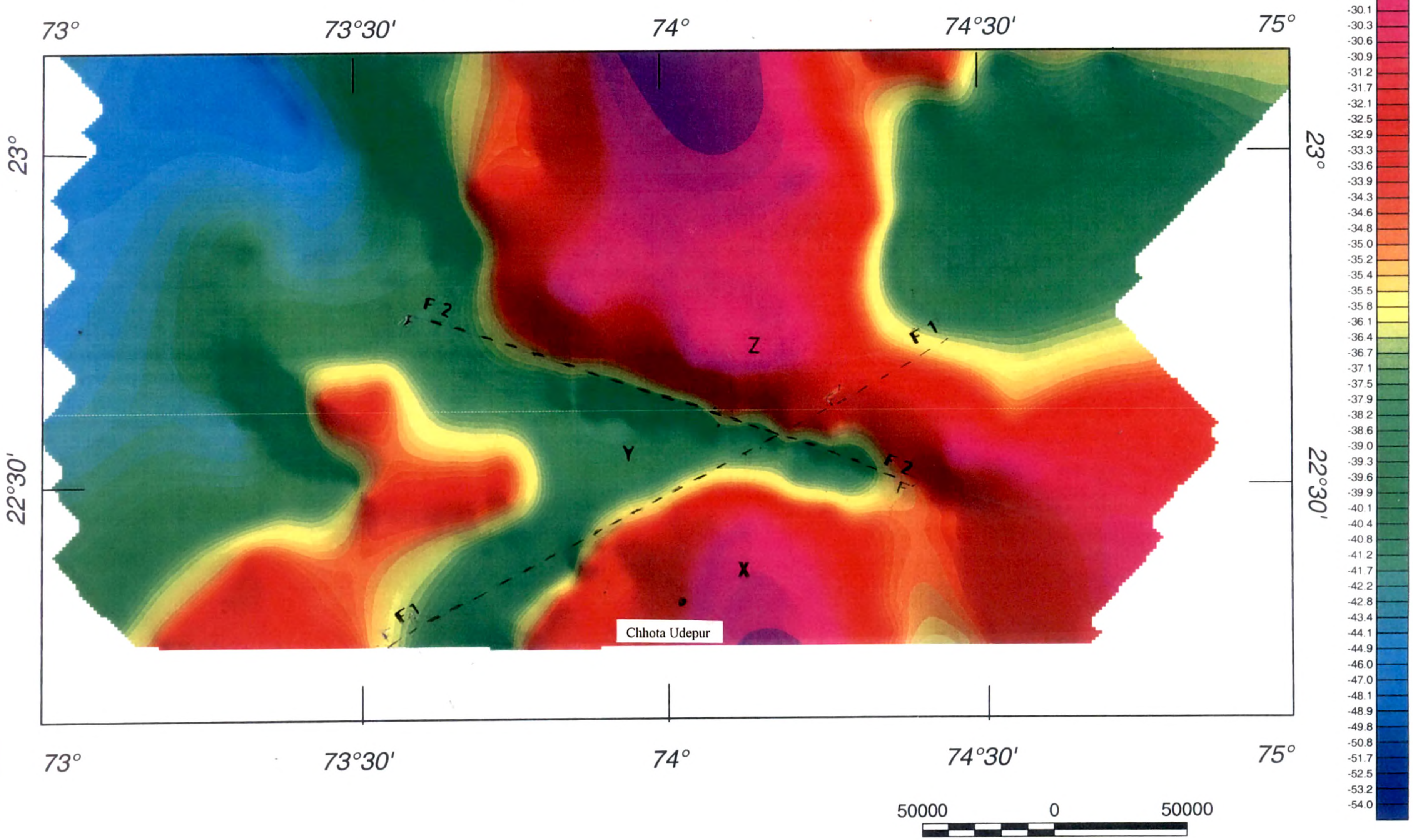

Fig 4.5

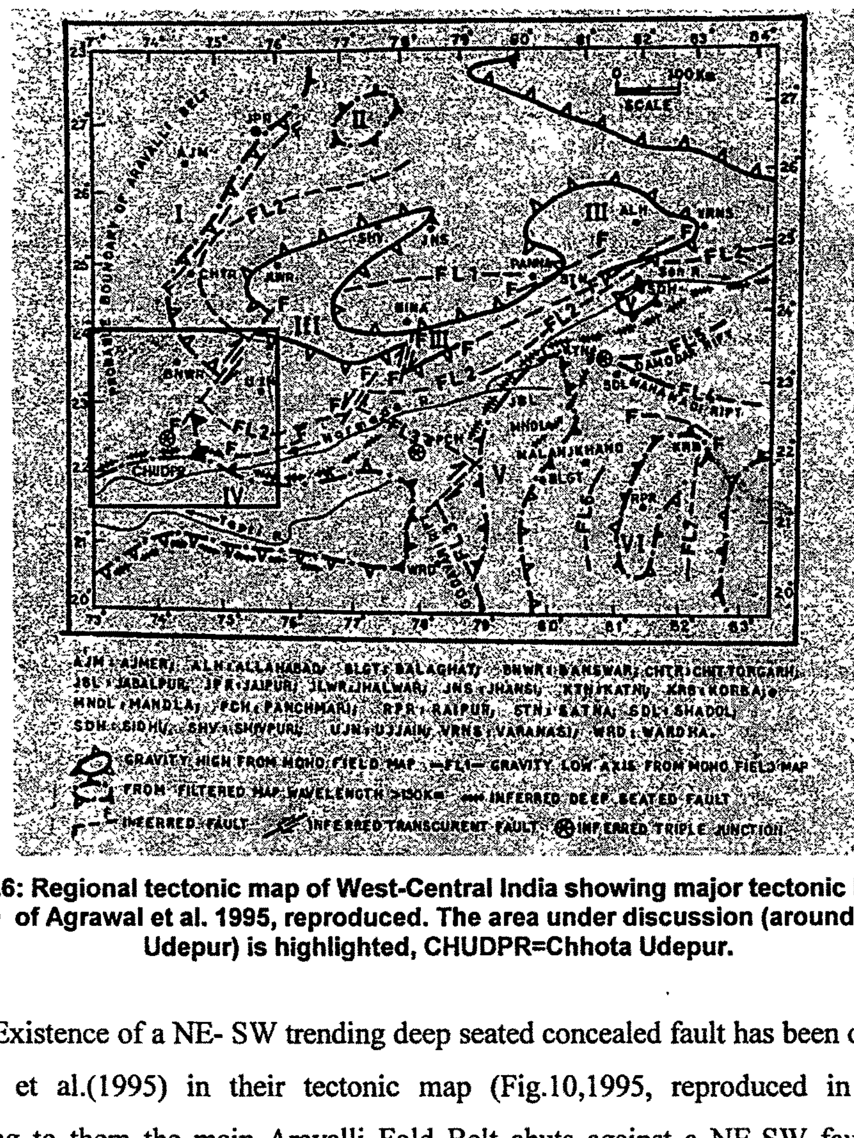

Fig 4.6: Regional tectonic map of West-Central India showing major tectonic blocks: Fig.10 of Agrawal et al. 1995, reproduced. The area under discussion (around Chhota Udepur) is highlighted, CHUDPR=Chhota Udepur.

Existence of a NE- SW trending deep seated concealed fault has been detected by Agrawal et al.(1995) in their tectonic map (Fig.10,1995, reproduced in **Fig 4.6**). According to them the main Aravalli Fold Belt abuts against a NE-SW fault (located between BNWR and UJN in their map (**Fig 4.6**). They have identified in all six tectonic blocks in Western and Central Indian Craton (Block I–VI, **Fig. 4.6**). They have also shown a triple junction north of Chhota Udepur (22°30'E: 74°00'), uniting Block I, Block III and Block IV. The Aravalli Mountain Belt is shown to represent Block- I, whereas Satpura Mobile belt comprises block-IV. This map clearly indicates that the tectonic setting of Chhota Udepur region differs from Aravalli Mountain Belt. Thus the author assumes that the Pre-Champaner Gneiss is a part of Palaeoproterozoic crustal block, which has been remobilised from time to time, and these crustal blocks have been affected by a strong tectonothermal event during 1168±30 Ma and it is also synchronous with the tectonothermal event imprinted in Satpura Mobile Belt (described by

Bandopadhyay et al, 1995). This geophysical aspects related to granite and granite gneiss are further discussed in detail in chapter 6, section 6.7.

4.6. STRUCTURAL SYNTHESIS

Various deformational phases, geometry, orientation and metamorphic events are given in **Table 4.2.** and the interference patterns of various folds are as given below. Study of mesoscopic folds, deformed lineations and structural analysis of area indicate that;

1. There are four episodes of folding in this region of which the early two (**D_1** and **D_2**) have produced folds of reclined nature (**F_1** and **F_2**) and the later two (**D3** and **D_4**) have resulted in open upright folds (F3 and **F_4**). **a**). Interference of F_2 folds on F_1 folds has resulted superimposed fold *type II* of Ramsay. **F_1** and **F_2** fold axes intersect at high angles (40° to 90°) and S_1 and S_2 intersect at low angles. Interference of **F_2** and **F_3** has resulted in the development of co-axial folds. **b**) However, superimposition of **F_1** and **F_3** folds on mesoscopic scale are rare. When present they are seen as hook shaped folds since **F_2** isoclinal folds and **F_3** upright folds are almost co-axial, e.g. near Wawadi (Fig. 4.6.).**c**) **F_3** and **F_4** are mutually perpendicular upright folds/warps with general E-W and N-S axial traces respectively.

2. Mesoscopic **F_1** and **F_2** folds in layers of different competency are of variable wavelength and disharmonic in nature, all indicate that they are products of buckling. In general the amplitude to wavelength ratio of both **F_1** and **F_2** folds are fairly high. The second event (**D_2**) has resulted in flexural slip folding (**F_2**).

3. **F_2** and **F_3** are co-axial as evidenced by the mesoscopic hook shaped folds and general pattern of lineations around **F_2** hinges. **D_3** resulted in buckle folding with post buckle flattening as evidenced from the **L_2** lineation pattern. Study of the map pattern and S_2 poles in different sectors indicate that **F_3** represent regional folds and their local manifestation is not as intense as the earlier folds. **D_4** is a weak and shallow depth deformation as indicated by their formation related to kink bands.

4. Mutually perpendicular nature of **F_1** and **F_2**- **F_3** indicate that the tectonic forces changed from E-W compressions in early period to N-S in later period during the Precambrian times and finally ended up with the intrusion of Godhra granite.

A comparison of folding events of Chhota Udepur area with the main Aravalli Fold belt exposed in Rajasthan reveals a striking difference in the orientation of folds (Table 4.2). Both areas have been affected by four phases of deformation of which early two events (**D_1** and **D_2**) have generated isoclinal reclined folds (**F_1** and **F_2**) intersecting at high angles and the later two events have produced upright folds (**F_3** and **F_4**). While in the main Aravalli Fold Belt the **F_1** folds are oriented E-W and **F_2** folds lie in NNE-SSW direction, in Chhota Udepur area the **F_1** folds plunge mainly towards N or S and **F_2** folds plunge mainly towards W or E. The open **F_3** folds in Aravalli Fold Belt lie in NNE-SSW direction, whereas in Chhota Udepur they lie in E-W direction. The **F_4** folds are coaxial with **F_2** and **F_3** (NNE-SSW) in Aravalli Fold Belt, whereas in Chhota Udepur **F_4** are coaxial with **F_1**, but not with **F_2** and **F_3**.(Table 4.3)

It implies that while in Rajasthan the initial tectonic forces changed from N-S compression during **D_1** to E-W (ENE-WSW) compression during **D_2** - **D_3**; in Chhota Udepur region it changed from initial E-W compression to N-S compression in the later stages (**D_2** and **D_3**) and then again to E-W compression during **D_4**.

Studying the diastrophic structures in field, comparing them and studying regional tectonics based on geophysical data it may be inferred that; a) The Banded Gneissic Complex of Aravalli Mountain belt is different from the Pre Champaner Gneisses, or b) Part of the Banded Gneissic Complex has been disrupted by NE-SW trending regional transcurrent fault also rotated around the triple junction, near north of Chhota Udepur (Fig. 7.2, after Agrawal et al, 1995) and subsequently remobilised under different tectonic setting. Thus the difference in orientation of folding patterns and regional tectonics indicates that the rocks of study area apparently appear to belong to a separate tectonic regime and not related to Aravalli tectonism.